MiR-1-3p Downregulation Delays Endochondral Ossification of the Acetabular Roof in DDH

Rui Ding
Nanchang University Second Affiliated Hospital
xijuan liu
Nanchang University Second Affiliated Hospital
jian zhang
Nanchang University Second Affiliated Hospital
jinghong yuan
Nanchang University Second Affiliated Hospital
sikuan zheng
Nanchang University Second Affiliated Hospital
xigao cheng
Nanchang University Second Affiliated Hospital
Jingyu Jia (jiaintong9@163.com)
Nanchang University Second Affiliated Hospital

Research Article

Keywords: Developmental dysplasia of the hip, microRNA, miR-1-3p, SOX9, Endochondral ossification

Posted Date: March 10th, 2021

DOI: https://doi.org/10.21203/rs.3.rs-281896/v1

Version of Record: A version of this preprint was published at Journal of Orthopaedic Surgery and Research on August 18th, 2021. See the published version at https://doi.org/10.1186/s13018-021-02666-1.

Abstract

Background: Developmental dysplasia of the hip (DDH) is a highly prevalent hip disease among children. However, its pathogenesis remains unclear. MiRNAs are important regulators in cartilage development. In previous study, miRNA high-throughput sequencing on an animal model of DDH showed a low level of miR-1-3p in the cartilage of acetabular roof (ARC), but its role in DDH pathogenesis was not addressed. Therefore, our aim was to investigate the effects of miR-1-3p in the ARC.

Methods: The X-ray examination was performed to confirm acetabular dysplasia, MRI imaging and HE staining was conducted to further evaluate the ARC thickness in each animal model. The FISH was used to confirm the expression of miR-1-3p in the ARC and chondrocytes. The target gene of miR-1-3p was predicted by bioinformatics database. The dual-luciferase reporter gene assay was used to confirm the targeting relationship between miR-1-3p and SOX9. The gene expression of miR-1-3p, SOX9, RUNX2 and collagen type X by QPCR analysis. The relative proteins level was detected by western blot analysis. The level of SOX9, RUNX2 and collagen type X in the ARC through immunohistochemistry analysis. Alizarin Red S staining was used to observe the mineralized nodules produced by chondrocytes.

Results: The low expression of miR-1-3p in the ARC of DDH. SOX9 is miR-1-3p target gene. Downregulation the expression of miR-1-3p in vitro and demonstrated significantly reduced chondrocytes generated mineralized nodules, as opposed to the control. We also confirmed that, with miR-1-3p silencing, SOX9 expression was upregulated, whereas expression of genes associated with endochondral osteogenesis RUNX2 and collagen type X were downregulated. To confirm the involvement of miR-1-3p silencing in abnormal ossification through SOX9, we also performed a rescue experiment where SOX9 silencing restored the low expression of RUNX2 and collagen type X, produced by miR-1-3p downregulation. Lastly, the elevated SOX9 levels and reduced RUNX2 and collagen type X levels in the ARC of DDH rabbits were also verified, using immunohistochemistry, RT-PCR, and western blot.

Conclusion: The low expression of mir-1-3p in the ARC of DDH, which may be the cause of the acetabular roof abnormal endochondral ossification in DDH.

Introduction

Developmental dysplasia of the hip (DDH) is a highly prevalent three-dimensional deformity among children [1]. Despite prompt treatment, either conservatively or surgically, some infants and children can still develop residual acetabular dysplasia, which can progress to form severe osteoarthritis in adulthood, making the need for a total hip replacement inevitable [2, 3]. In children, the acetabulum is mainly composed of ilium, ischium, pubis, and Y-shaped epiphyseal plate (triradiate cartilage), wherein the ilium forms the acetabular roof and the pubis and ischium constitutes the anterior and posterior walls of the acetabulum, respectively [4–6]. Using the 3DCT split technique, we found developmental defects on the lateral side of the acetabular roof and the acetabular index increased in children with untreated DDH. In addition, the ischium was rotated, promoting increased forward inclination of the acetabulum [4–6]. In

treated DDH children, however, in a period of 10–59 months, we found all structural defects, namely, developmental defects on the anterior wall of the acetabulum, thickening of the posterior and medial walls, rotation of the ischium, and forward inclination of the acetabulum return to normal. However, some children still exhibited developmental defects in the acetabular roof, and the tilt angle remained high [7]. In work done by Mootha et al [8], involving 45 DDH children aged 12–48 months, it was also shown that the acetabular anteversion was increased in DDH children, relative to healthy aged-matched children. This was consistent with other studies which also showed a marked association between developmental defect of the acetabular roof and DDH [9, 10].

To reveal the pathogenesis behind acetabular roof developmental defect in children with DDH, we established a DDH animal model by straightening and swaddling the legs of New Zealand white rabbits [11, 12]. We observed that the acetabular roof cartilage (ARC) was thicker on the side where the limb was straightened, i.e. the DDH side, as compared to the untreated control side. This phenomenon was also reported by Li et al [12]. Our MRI results was also similar to MRI observations of children with DDH. Moreover, in a previous study, the acetabular roof developmental defect, seen in the DDH models, originates from abnormal cartilage ossification is the cause of the developmental defect of acetabular roof [13].

MiRNAs are 21–24 nucleotides long, highly conserved, non-coding (nc) RNA molecules. They function by sequence pairing with the 3’-non-coding region of the target mRNA molecules to suppress translation and drive degradation of the mRNAs [14]. According to bioinformatics studies, approximately a third of all human mRNAs are subject to regulation by miRNAs [15]. Recent evidences suggest that the abnormal expression of miRNAs is strongly associated with proliferation, differentiation, apoptosis, and development of chondrocytes [16–20]. To examine the role of miRNA in the thickening of the acetabular roof cartilage in DDH, differential miRNA expression was analyzed in the acetabular roof cartilage of DDH models verses untreated controls. Based on the results from the miRNA microarray, 18 miRNAs were differentially expressed, including 3 high expression miRNAs and 15 low expression miRNAs [13]. In subsequent experiments, it was confirmed that the miRNA miR-129-5p regulated GDF11 expression to modulate Smad3/ IHH-induced endochondral ossification in the acetabular cartilage of DDH model [13].

To further elucidate the role of other miRNAs in DDH pathogenesis, this study performed QPCR verification and discovered very low expression of mir-1-3p, which was in accordance to our previous miRNA chip data. Considering the lack of studies on the expression and the mechanism of action of mir-1-3p in the epiphyseal plate (growth plate), this study aimed to explore mir-1-3p levels in the growth plate and examine its underlying mechanism of action in the pathogenesis of DDH.

Material And Methods

Establishment of the experimental animal model of DDH

30 four-week-old, healthy, New Zealand white rabbits (Nanchang Longping Domestic Rabbit Industry, Jiangxi Province, China), weighing 430–640 g, were used to induce DDH by fixing the left hind limbs in a straight position, while the right hind limbs were left untreated to serve as controls (Fig. 1). The animals were fed and maintained in a room with a temperature of 23°C and 50% humidity. The room was cleaned every other day. New feed (purchased from Lanling Hekangyuan Feed, China) and purified water were added to cages every two days to feed the rabbits until 8 weeks of age. At 8 weeks of age, X-ray examination was performed to confirm acetabular dysplasia, using the previous X-ray indicators [21], and MRI imaging was conducted to further evaluate the ARC thickness in each animal model. The evaluations of the acetabular dysplasia and the ARC thickness were carried out by two individual orthopedic physicians. Statistical data analysis was performed by other researchers. These evaluations adopted a single-blinded design; i.e., those evaluating the data were not informed which data came from which experimental group. This study was approved by the Ethics Committee of the Second Affiliated Hospital of Nanchang University in Jiangxi Province, China. ([2017] No. (091)).

Hematoxylin and eosin staining

The hip joint specimens were placed in 10% EDTA for decalcification for 4 weeks. Next, the specimens were cut to expose the coronal surface of the hip joint, as depicted in Fig. 1B (red line), and embedded in paraffin. The paraffin-embedded specimens were then cut into 4-μm-thick sections, placed on glass slides, dewaxed in xylene solution, hydrated, and stained with hematoxylin dye for 1 min. Next, the sections were washed and placed in hydrochloric acid alcohol solution for differentiation, followed by bluing in Scott’s solution for 3 min, washing, and staining with eosin dye for 10 min. The sections were then dehydrated in graded ethanol solutions and mounted with neutral resin, followed by overnight (O/N) drying at 65°. Lastly, the stained sections were photographed under a light microscope at 100X magnification and the cartilage thickness was measured using Image-pro plus 6.0 software (Media Cybernetics, Inc., Rockville, MD, USA).

Bioinformatics prediction

TargetScan (http://www.targetscan.org/vert_71/) was used to speculate downstream target genes of mir-1-3p.

Dual-luciferase reporter gene assay

miR-1-3p mimic (WT), miR-1-3p mutant (MUT), and negative control (NC) were co-transfected into human primary chondrocytes together with the Sox9 3'UTR luciferase reporter plasmid (GenScript) and renilla reporter contol. After 48h, the cells were harvested using Dual-Lumi™ II Luciferase Reporter Assay kit (Beyotime Institute of Biotechnology), in accordance with manufacturer's instructions and the luciferase activity was detected using a multimode reader (BioTek Instruments, Inc.). The Firefly luciferase activity was normalized using Renilla luciferase activity.

Chondrocyte culture

The ARC was chopped and digested with 0.25% trypsin at 37°C for 30 min, followed by culturing in serum-free DMEM with 0.2% type II collagenase for 4 hrs. The isolated rabbit chondrocytes were subsequently sub-cultured in complete DMEM (Gibco, Waltham, MA) with 10% fetal bovine serum (FBS) and 1% penicillin/streptomycin (PS) in a humid environment with 5% CO2 at 37°C for future experiments. Human primary chondrocytes were purchased from Procell Life Science & Technology Co.,Ltd. (Wuhan, Hubei Province, China) were cultured in complete DMEM with 10% FBS and 1% PS in an incubator with 5% CO2 at 37°C.

Transfection

At 80–90% confluency, mir-1-3p inhibitor, NC-miRNA inhibitor, SOX9 siRNA, or siNC messenger RNA (mRNA) (RiboBio, Guangzhou, Guangdong Province, China) were transfected into human primary chondrocytes using Lipofectamine 3000 reagent, following manufacturer's guidelines (Invitrogen, Carlsbad, CA) and cultured in serum-free DMEM for 6 hours, followed by culturing in DMEM with serum for 72 hours. These cells were next used for further experiments.

RNA extraction and qPCR

Total RNAs was isolated from either the ARCs of 7 rabbits or cultured chondrocytes using Trizol reagent (Invitrogen, Waltham, MA). Next, they were reverse transcribed using the PrimeScript™RT reagent Kit with gDNA Eraser kit (Takara Bio, Kusatsu, Japan). The extracted total RNA was then quantified using the ABIQ6PCR system. The miRNAs primers were designed by RiboBio (Guangzhou, Guangdong Province, China) and summarized in Table 1. All experiments were performed 3X and the average of the results are represented in this paper.

Western blotting

Total protein was isolated from either the ARC of 7 rabbits or cultured chondrocytes using RIPA lysis buffer (Applygen Technologies Inc., Beijing, China) and were quantified using the bicinchoninic acid (BCA) protein assay kit (Pierce Biotechnology, Rockford, IL), followed by separation using sodium dodecyl sulfate polyacrylamide gel electrophoresis (SDS-PAGE) and subsequent transfer of proteins to the polyvinylidene difluoride (PVDF) membranes. Next, the PVDF membranes were labeled with primary antibodies (1:1000; CST Biological Reagents Company Limited, Shanghai, China) O/N at 4°C, followed by phosphate-buffered saline (PBS)-wash 3X, incubation with immunoglobulin G-horseradish peroxidase (IgG-HRP)-conjugated secondary antibodies (1:2000; Beijing Golden Bridge Biotechnology, Beijing, China) at room temperature (RT) 1 h, PBS-wash 3X, and color development using chemiluminescent HRP substrate. GAPDH served as an endogenous control. All experiments were performed 3X and the best representation of the results are represented in this paper.

Alizarin Red S staining

The cell culture medium was discarded and the cells were PBS-washed 2X before fixing in 4% paraformaldehyde for 15 min, followed by double distilled water-wash 3X, and stain in ARS solution (Beijing Solarbio Science & Technology, Beijing, China) for 30 min. Subsequently, the cells were double

distilled water-washed again before observation under a light microscope. The ARS stain colored the calcium nodules deep orange red.

Immunohistochemistry

The paraffin-embedded, 4-μm-thick sections were mounted on glass slides. Next, the paraffin was removed and the sections were hydrated to retrieve antigens before independent labeling with primary antibodies (Beijing Biosynthetic Biotechnology, Beijing, China) in 1:200 concentrations. Following wash, the sections were labeled with 1:200 goat anti-rabbit IgG-HRP secondary antibodies (Beijing Golden Bridge Biotechnology), followed by conventional color development reagent, and observed and photographed under a light microscope at 200X. 5 random visual fields were selected per treatment group for analysis. Image-pro plus 6.0 software (Media Cybernetics, Inc., Rockville, MD, USA) was employed to analyze the stained cells in each image, using the same parameters. The accumulated optical density (IOD) and the pixel area (area) of each photo were recorded and the average IOD / area (mean density) was calculated.

Fluorescence in situ hybridization

The sections of paraffin-embedded acetabular samples and chondrocytes were incubated with 500 ng/ml FAM-labeled probes for 48 hours using a FISH kit (Shanghai Gefan Biotechnology, Shanghai, China). Mir-1-3p expression was then recorded under a fluorescence microscope and further analyzed using Image J (version 1.48v).

Statistical analysis

All data are expressed as mean ± standard deviation. Following outlier removal, the paired t test was employed to compare expression of relevant genes and proteins between DHH samples and controls. One-way analysis of variance (ANOVA) with post-hoc Tukey's test was used to compare the expression of relevant genes and proteins in chondrocytes treated with blank control, normal control, miR-1-3p mimic, si-mir-1-3p, and si-SOX9. Statistical significance was considered at P-value < 0.05. The SPSS 25.0 software and Prism software were used to perform statistical analysis.

Results

DDH rabbits exhibited thick ARC and low miR-1-3p expression

To examine the pathogenesis of DDH, we successfully induced DDH in 18 rabbits. Upon euthanasia, tissue specimens were collected from the hip joint of all rabbits. In particular, ARC samples from 14 left acetabular dysplasia and 14 right controls (14 DDH rabbits) were used for RNA and protein examination, whereas ARC samples from 4 left acetabular dysplasia and 4 right controls (4 DDH rabbits) were used in HE staining, immunohistochemistry, and FISH investigation.

In this study, X-ray imaging confirmed the successful establishment of DDH in New Zealand white rabbits (Fig. 2A). Moreover, the ARC was remarkably thick in the DDH rabbits, as evidenced by gross specimen observation, MRI images, and HE staining (Fig. 2B-D).

Next, we confirmed miR-1-3p expression in the acetabular roof cartilage by FISH (Fig. 2E), followed by verification of low mir-1-3p levels in the DDH acetabular roof cartilage verses healthy controls, using qPCR (Fig. 2F). This result was consistent with our previously conducted miRNA chip data [10].

MiR-1-3p downregulation inhibits chondrocytes hypertrophy and reduces mineralization

First, we confirmed low miR-1-3p levels in human and rabbit chondrocytes, using immunofluorescence (Fig. 3A). Next, we incorporated primary human chondrocytes with a miR-1-3p inhibitor to ascertain the specific role of miR-1-3p in chondrocytes. As shown in Fig. 3B, miR-1-3p levels fell dramatically upon transfection with the miR-1-3p inhibitor ($P < 0.01$). To assess whether low miR-1-3p levels promotes abnormal chondrocyte ossification, we performed ARS staining to detect calcium deposits in these cells. The miR-1-3p inhibited cells exhibited reduced mineralization, as compared with control (Fig. 3C). We, also, analyzed the gene expression of endochondral osteogenesis markers RUNX2 and collagen type X and showed a substantial decrease in the expression of both genes, suggesting reduced osteogenesis (Fig. 3D and 3E, $P < 0.05$).

MiR-1-3p directly targets SOX9

Our prior bioinformatics analysis revealed SOX9 as a downstream target gene of miR-1-3p (Fig. 4A). We further confirmed this, using a luciferase reporter assay, where SOX9-WT and miR-1-3p mimics incorporated cells showed reduced luciferase activity, but the activity was restored in miR-1-3p mimics and SOX9-mut incorporated cells (Fig. 4B, $P < 0.05$). Alternately, miR-1-3p suppression, using miR-1-3p inhibitors, in chondrocytes resulted in dramatic increases in SOX9 transcript and protein expression (Fig. 4C and 4D, $P < 0.01$). These results suggest a strong modulatory relationship between miR-1-3p and Sox9.

MiR-1-3p suppression inhibits chondrocyte hypertrophy and reduces mineralization via SOX9

Given that miR-1-3p suppression can elevate SOX9 expression and lower RUNX2 and collagen type X expression, we next examined the role of miR-1-3p in chondrocyte hypertrophy and reduced mineralization through Sox9. To do this, we simultaneously incorporated human chondrocytes with mir-1-3p inhibitor and si-SOX9. Using RT-PCR and western blot analysis, we verified reduced expression of mir-1-3p and SOX9 in the cells, which resulted in an increased expression of RUNX2 and type X collagen transcripts and proteins, as opposed to controls (Fig. 5A-C, $P < 0.05$). Furthermore, we confirmed the high SOX9 expression and low RUNX2 and type X collagen levels in acetabular roof cartilage DHH model vs healthy controls, as evidenced by immunohistochemistry, qPCR, and western blot analysis (Fig. 6A-C, $P < 0.05$).

Discussion

Multiple reports have suggested that the increased thickness of the acetabular roof cartilage, in DDH children and animal models, is associated with delayed endochondral ossification [10, 13, 22, 23]. This study has successfully induced DDH in New Zealand white rabbits. We also demonstrated that the MRI manifestation of the rabbit DDH acetabular roof is similar to the MRI data from DDH children, especially in terms of producing a thicker acetabular roof cartilage (also confirmed using gross specimen inspection and HE staining).

Growing evidences suggest a crucial role of miRNA in cartilage physiology [24]. Miyaki et al.[16], for instance, discovered the presence of miR-140 in the growth plate of X, which modulates target gene Adamts-5, an important matrix protease that hydrolyzes proteoglycans and type II collagen, to maintain healthy cartilage structure and function. Alternately, miR-140-knockout mice developed severe osteoarthritis. Nakamura et al. [17], on the other hand, demonstrated, using miR-140-knockout mice, that the Dnpep-mediated bone morphogenetic protein (BMP) signaling pathway was affected, which stimulated articular chondrocytes differentiation into hypertrophic chondrocytes and, thus, developed chondrogenic disorder. Likewise, Kobayashi et al. [18], specifically knocked out the Dicer gene in a mouse model which dramatically reduced miRNAs expression in chondrocytes and strongly suppressed bone formation and chondrocyte proliferation in the growth plate. Similarly, Zhang et al. [19], confirmed the low expression of miR-150-5p in osteoarthritis, which negatively impacted AKT Serine/Threonine Kinase 3 (AKT3) pathway to promote chondrocyte proliferation and inhibit apoptosis and degradation of extracellular matrix in chondrocytes. In another example, Bluhm et al. [20], reported high miR-332 expression, which modulated the RAF/MEK/ERK pathway to upregulate chondrocyte differentiation and develop achondroplasia. Taken together, miRNA not only modulates chondrocyte proliferation, differentiation, apoptosis, endochondral ossification, and cartilage development, but also osteoarthritis and achondroplasia [16–20]. However, as a member of miRNA, the expression and function of mir-1-3p in chondrocytes have not been elucidated, and its mechanism of action in acetabulum abnormal endochondral ossification in DDH remained unknown.

Based on existing research, miR-1-3p is a tumor-related miRNA that is involved in the viability, proliferation, and apoptosis of multiple cancerous cells. In fact, miR-1-3p was shown to be severely down-regulated in gastric cancer and its mechanism of action was shown to include negative regulation of STC2 to suppress cell proliferation and invasion to form gastric cancer [25]. Similarly, Gao et al. [26], reported that miR-1-3p can suppress BDNF expression and phosphorylation of TrkB to halt proliferation and invasion of bladder cancer cells. Likewise, Zhang et al. [27], confirmed low levels of miR-1-3p in hepatocellular carcinoma cell lines, which improved Sox9 expression, cell proliferation, and suppressed apoptosis in HCCLM3 and Bel-7474 cells. In addition, myogenic factors like MyoD, Mef2, and SRF were reported to increase miR-1-3p expression, whereas skeletal muscle hypertrophy decreased miR-1-3p expression [28, 29]. Moreover, in a recent study involving Chinese osteoporotic patients, miR-1-3p was reported to be significantly downregulated and SFRP1 was upregulated with reduced bone formation and bone mass [30]. In this study, we demonstrated low miR-1-3p levels in the ARC of DDH rabbits,which is

consistent with the high-throughput sequencing data we conducted previously[13]. To ascertain the function of miR-1-3p in chondrocytes, we first confirmed its expression in normal human and rabbit chondrocytes, using FISH. We also demonstrated that with low miR-1-3p levels, in these chondrocytes, there also existed mineralized nodules, as evidenced by ARS staining. Analysis of endochondral osteogenesis-related genes showed reduced expression of RUNX2 and collagen type X following miR-1-3p suppression. To identify downstream targets of miR-1-3p, we screened out bioinformatics data and found SOX9. SOX9 is normally expressed in all chondrogenic progenitors and chondrocytes of the articular cartilage throughout adulthood and is a master transcription factor regulating multiple events involving chondrogenesis [31–34]. Moreover, several studies suggested a role of SOX9 in endochondral ossification. In particular, SOX9 suppression in the normal growth plate is essential for endochondral ossification, whereas high expressing Sox9 in the growth plate retards this process [35, 36]. In accordance with other studies, we showed a significant upregulation of SOX9 in mir-1-3p-silenced chondrocytes in vitro. To confirm whether miR-1-3p downregulation reduces RUNX2 and collagen type X expression via SOX9, we performed rescue experiments. In brief, we demonstrated that SOX9 silencing restored RUNX2 and collagen type X expression in cells treated with miR-1-3p inhibitor verses control. Prior studies have reported that Sox9 negatively regulates Runx2 and type X collagen expression in order to modulate endochondral ossification-related disorders [36, 37]. To verify the miR-1-3p-mediated regulation of endochondral ossification genes, the levels of SOX9, RUNX2, and collagen type X were examined in the ARC of DDH and healthy rabbit acetabula, using immunohistochemistry, qPCR, and western blot analysis. As expected, our results showed that low miR-1-3p levels in the ARC resulted in high expression of SOX9 and low expression level of RUNX2 and collagen type X in the DDH rabbit acetabula verses controls. These results suggest a strong involvement of miR-1-3p in the modulation of abnormal endochondral ossification of the ARC in DDH.

Conclusion

In summary, we demonstrated, for the first time, that miR-1-3p modulates abnormal endochondral ossification of the ARC in DDH via its regulation of the target gene SOX9. In the future, our findings need to be verified in vivo; particularly, the dynamic alterations in miR-1-3p expression in the growth plate during the embryonic, neonatal, and childhood stages. We also suggest the establishment of an in vivo gene knockout for further research advances in this field.

Abbreviations

DDH, developmental dysplasia of the hip; ARC, acetabular roof cartilage; CT, computed tomography; MRI, magnetic resonance imaging; 3DCT, three-dimensional CT; MiRNA, microRNA; QPCR, quantitative polymerase chain reaction; HE, hematoxylin and eosin; ARS, Alizarin Red S; FISH, fluorescence *in situ* hybridization; NC, normal control; ARS, Alizarin Red S; SOX9, SRY-Box transcription factor 9; Runx2, Runt-related transcription factor 2; Col 10, collagen type X;

Declarations

Ethics approval and consent to participate

This study was approved by the Ethics Committee of the Second Affiliated Hospital of Nanchang University in Jiangxi Province, China. ([2017] No. (091)).

Consent for publication

Not applicable.

Availability of data and materials

Please contact author for data requests.

Competing interests

All authors have no conflicts of interest.

Funding

This work was supported by National Nature Science Foundation of China (NO.81360268 and NO.81960392).

Author contributions

JJ and RD conceived and designed the experiments. XL, JZ, and JY performed the experiments. SZ and XC analysed the data. JJ and RD wrote the main manuscript text.

Acknowledgements

The authors thank Shen Hu and Dingwen He in the management of experimental animals.

References

1. Tréguier C, Chapuis M, Branger B. Developmental dysplasia of the hip. J Radiol. 2011; 92(6):481-93.
2. Chen Y, Lv H, Li L, Wang E, Zhang L, Zhao Q. Expression of PAPP-A2 and IGF Pathway-Related Proteins in the Hip Joint of Normal Rat and Those with Developmental Dysplasia of the Hip. Int J Endocrinol. 2019; 2019:7691531.
3. Morita D, Hasegawa Y, Seki T, Amano T, Takegami Y, Kasai T, Higuchi Y, Ishiguro N. A Possible New Radiographic Predictor of Progression of Osteoarthritis in Developmental Dysplasia of the Hip: The Center Gap. Clin Orthop Relat R. 2018; 476(11):2157-66.
4. Jia J, Li L, Zhang L, Zhao Q, Wang E, Li Q. Can excessive lateral rotation of the ischium result in increased acetabular anteversion? A 3D-CT quantitative analysis of acetabular anteversion in

children with unilateral developmental dysplasia of the hip. Journal of Pediatric Orthopedics. 2011; 31(8):864-9.

5. Jia J, Li L, Zhang L, Zhao Q, Liu X. Three dimensional-CT evaluation of femoral neck anteversion, acetabular anteversion and combined anteversion in unilateral DDH in an early walking age group. Int Orthop. 2012; 36(1):119-24.
6. Jia J, Zhang L, Zhao Q, Li L, Liu X. Does medial rotational deformity of the whole pelvis universally exist in unilateral DDH? Arch Orthop Traum Su. 2011; 131(10):1383-8.
7. Liu X, Cheng X, Jia J. Evaluating acetabular version through MRI and CT in 55 children of untreated DDH and 222 normal children. Int J Clin Exp Med. 2019; 12:201–211.
8. Mootha AK, Saini R, Dhillon MS, Aggarwal S, Kumar V, Tripathy SK. MRI evaluation of femoral and acetabular anteversion in developmental dysplasia of the hip. A study in an early walking age group. Acta Orthop Belg. 2010; 76(2):174-80.
9. Jacobsen S, Rømer L, Søballe K. The other hip in unilateral hip dysplasia. Clinical Orthop Relat Res. 2006; 446:239-46.
10. Lu W, Li L, Zhang L, Li Q, Wang E. Development of acetabular anteversion in children with normal hips and those with developmental dysplasia of the hip: a cross-sectional study using magnetic resonance imaging. Acta orthop. 2021:1-6.
11. Michelsson JE, Langenskiöld A. Dislocation or subluxation of the hip. Regular sequels of immobilization of the knee in extension of young rabbits. The Journal of Bone and Joint Surgery American Volume. 1972; 54(6):1177-86.
12. Li TY, Ma RX. Increasing thickness and fibrosis of the cartilage in acetabular dysplasia: a rabbit model research. Chinese Medical Journal. 2010; 123(21):3061-6.
13. Liu X, Deng X, Ding R, Cheng X, Jia J. Chondrocyte suppression is mediated by miR-129-5p via GDF11/SMAD3 signaling in developmental dysplasia of the hip. J orthop Res. 2020; 38(12):2559-72.
14. Alberti C, Manzenreither RA, Sowemimo I, Burkard TR, Wang J, Mahofsky K, Ameres SL, Cochella L. Cell-type specific sequencing of microRNAs from complex animal tissues. Nat Meth. 2018; 15(4):283-9.
15. Lewis BP, Burge CB, Bartel DP. Conserved seed pairing, often flanked by adenosines, indicates that thousands of human genes are microRNA targets. Cell. 2005; 120(1):15-20.
16. Miyaki S, Sato T, Inoue A, Otsuki S, Ito Y, Yokoyama S, Kato Y, Takemoto F, Nakasa T, Yamashita S, et al. MicroRNA-140 plays dual roles in both cartilage development and homeostasis. Genes Develop. 2010; 24(11):1173-85.
17. Nakamura Y, Inloes JB, Katagiri T, Kobayashi T. Chondrocyte-specific microRNA-140 regulates endochondral bone development and targets Dnpep to modulate bone morphogenetic protein signaling. Mol Cell Biol. 2011; 31(14):3019-28.
18. Kobayashi T, Lu J, Cobb BS, Rodda SJ, McMahon AP, Schipani E, Merkenschlager M, Kronenberg HM. Dicer-dependent pathways regulate chondrocyte proliferation and differentiation. P NatL Acad Sci USA. 2008; 105(6):1949-54.

19. Zhang Y, Wang F, Chen G, He R, Yang L. LncRNA MALAT1 promotes osteoarthritis by modulating miR-150-5p/AKT3 axis. Cell Biosci. 2019; 9:54.
20. Bluhm B, Ehlen HWA, Holzer T, Georgieva V, Heiling J, Pitzler L, Etich J, Bortecen T, Frie C, Probst K. et al. miR-322 stabilizes MEK1 expression to inhibit RAF/MEK/ERK pathway activation in cartilage. Development. 2017; 144(19):3562-77.
21. Zhang X, Meng Q, Ma R, Chen G, Cheng L, Shen J. Early acetabular cartilage degeneration in a rabbit model of developmental dysplasia of the hip. Int J Clinl Exp Med. 2015; 8(8):14505-12.
22. Li LY, Zhang LJ, Li QW, Zhao Q, Jia JY, Huang T. Development of the osseous and cartilaginous acetabular index in normal children and those with developmental dysplasia of the hip: a cross-sectional study using MRI. The Journal of bone and joint surgery British volume. 2012; 94(12):1625-31.
23. Soboleski DA, Babyn P. Sonographic diagnosis of developmental dysplasia of the hip: importance of increased thickness of acetabular cartilage. Am J Roentgenol. 1993; 161(4):839-42.
24. Swingler TE, Niu L, Smith P, Paddy P, Le L, Barter MJ, Young DA, Clark IM. The function of microRNAs in cartilage and osteoarthritis. Clin Exp Rheumatol. 2019; 120(5):40-7.
25. Ke J, Zhang BH, Li YY, Zhong M, Ma W, Xue H, Wen YD, Cai YD. MiR-1-3p suppresses cell proliferation and invasion and targets STC2 in gastric cancer. Eur Rev Med Pharmacol Sci. 2019; 23(20):8870-7.
26. Gao L, Yan P, Guo FF, Liu HJ, Zhao ZF. MiR-1-3p inhibits cell proliferation and invasion by regulating BDNF-TrkB signaling pathway in bladder cancer. Neoplasma. 2018; 65(1):89-96.
27. Zhang H, Zhang Z, Gao L, Qiao Z, Yu M, Yu B, Yang T. miR-1-3p suppresses proliferation of hepatocellular carcinoma through targeting SOX9. OncoTargets Ther. 2019; 12:2149-57.
28. McCarthy JJ, Esser KA. MicroRNA-1 and microRNA-133a expression are decreased during skeletal muscle hypertrophy. J Appl Physiol. 2007; 102(1):306-13.
29. Callis TE, Deng Z, Chen JF, Wang DZ. Muscling through the microRNA world. Exp Biol Med. 2008; 233(2):131-8.
30. Gu H, Shi S, Xiao F, Huang Z, Xu J, Chen G, Zhou K, Lu L, Yin X. MiR-1-3p regulates the differentiation of mesenchymal stem cells to prevent osteoporosis by targeting secreted frizzled-related protein 1. Bone. 2020; 137:115444.
31. Kozhemyakina E, Lassar AB, Zelzer E. A pathway to bone: signaling molecules and transcription factors involved in chondrocyte development and maturation. Development. 2015; 142(5):817-31.
32. Symon A, Harley V. SOX9: A genomic view of tissue specific expression and action. Int J Biochem Cell Biol. 2017; 87:18-22.
33. Lefebvre V, Dvir-Ginzberg M. SOX9 and the many facets of its regulation in the chondrocyte lineage. Connect Tissue Res. 2017; 58(1):2-14.
34. Zhao Q, Eberspaecher H, Lefebvre V, Crombruggle B. Parallel expression of Sox9 and Col2a1 in cells undergoing chondrogenesis. Developmental dynamics : an official publication of the American Association of Anatomists. 1997; 209(4):377-86.

35. Hattori T, Müller C, Gebhard S, Bauer E, Pausch F, Schlund B, Bösl MR, Hess A, Surmann-Schmitt C, von der Mark H, et al. SOX9 is a major negative regulator of cartilage vascularization, bone marrow formation and endochondral ossification. Development. 2010; 137(6):901-11.
36. Cheng X, Li PZ, Wang G, Yan Y, Li K, Brand-Saberi B, Yang X. Microbiota-derived lipopolysaccharide retards chondrocyte hypertrophy in the growth plate through elevating Sox9 expression. J Cell Physiol. 2019; 234(3):2593-605.
37. Leung VY, Gao B, Leung KK, Melhado IG, Wynn SL, Au TY, Dung NW, Lau JY, Mak AC, Chan D et al. SOX9 governs differentiation stage-specific gene expression in growth plate chondrocytes via direct concomitant transactivation and repression. PLoS Genet. 2011; 7(11):e1002356.

Table

Table 1

Primer sequence for real-time quantitative PCR

Gene	Forward	Reverse
miR-1-3p	ACACTCCAGGTGGGTGGAATGT	CTCAACTGGTGTCGTGGAG
U6	CTCGCTTCGGCAGCACA	AACGCTTCACGAATTTGCGT
SOX9	GGCAAGCTCTGGAGACTTCTG	CTGCCCATTCTTCACCGACTT
RUNX2	GAATGCTTCATTCGCCTCACA	TGGCTGGATAGTGCATTCGT
COL10	CTCGTGGAAATGATGGTGCT	ACCAGGTTCACCGCTGTTAC
GAPDH	GGGCAGAGGAAGCTTCAGAAA	TCTCAGATGGATTCTGCGTGC

Figures

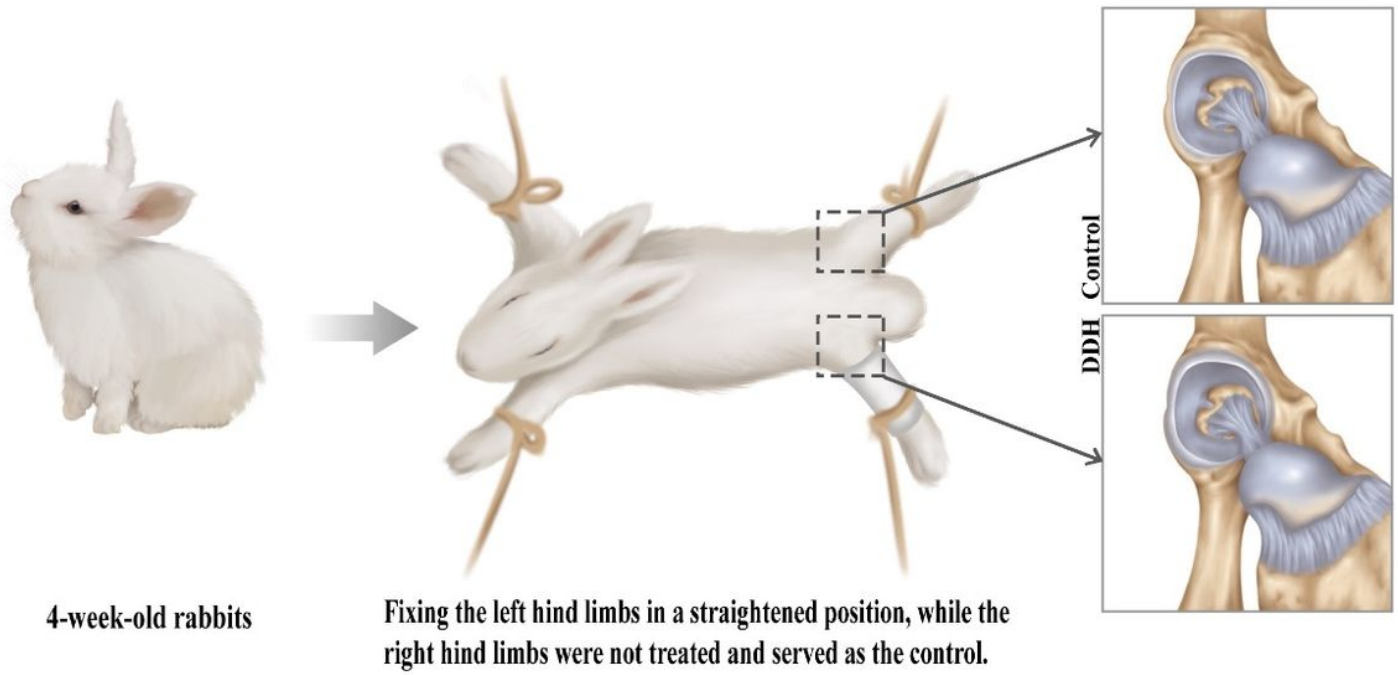

Figure 1

Schematic of the established DDH rabbit model 30 four-week-old rabbits were used to induce DDH by fixing the left hind limbs in a straight position, while the right hind limbs were left untreated and served as controls. The rabbits were given free access to food and water until 8 weeks of age, at which time the rabbit was euthanized for examination of the ARC. The ARC was found to be significantly thick in the DDH rabbits, as compared to the controls.

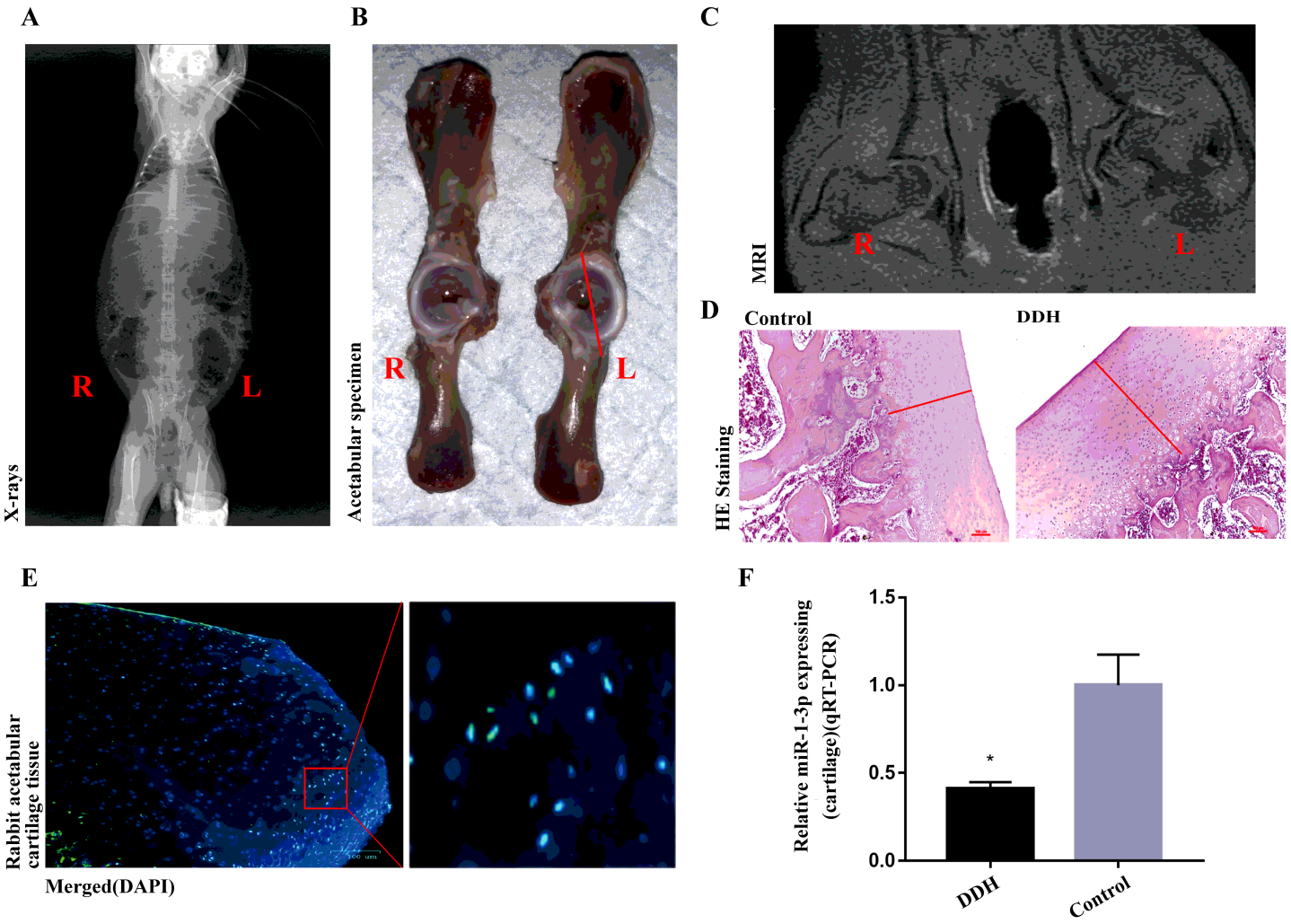

Figure 2

The DDH ARC was remarkably thick and had low miR-1-3p expression (A) The successful induction of DDH in the New Zealand white rabbits, as evidenced by X-ray. (B-D) The ARC in the DDH model was remarkably thick, compared to the untreated control limb, as evidenced by gross specimen observation, MRI imaging, and HE staining. Scale bar: 100 μm. (E) FISH was employed to detect mir-1-3p the mir-1-3p expressing in the sample of expression in DDH ARC. Scale bar: 100 μm. (F) QPCR confirmed the reduced mir-1-3p expression in the DDH ARC samples verses controls. (Data represents mean±SD, n=3 . *P<0.05).

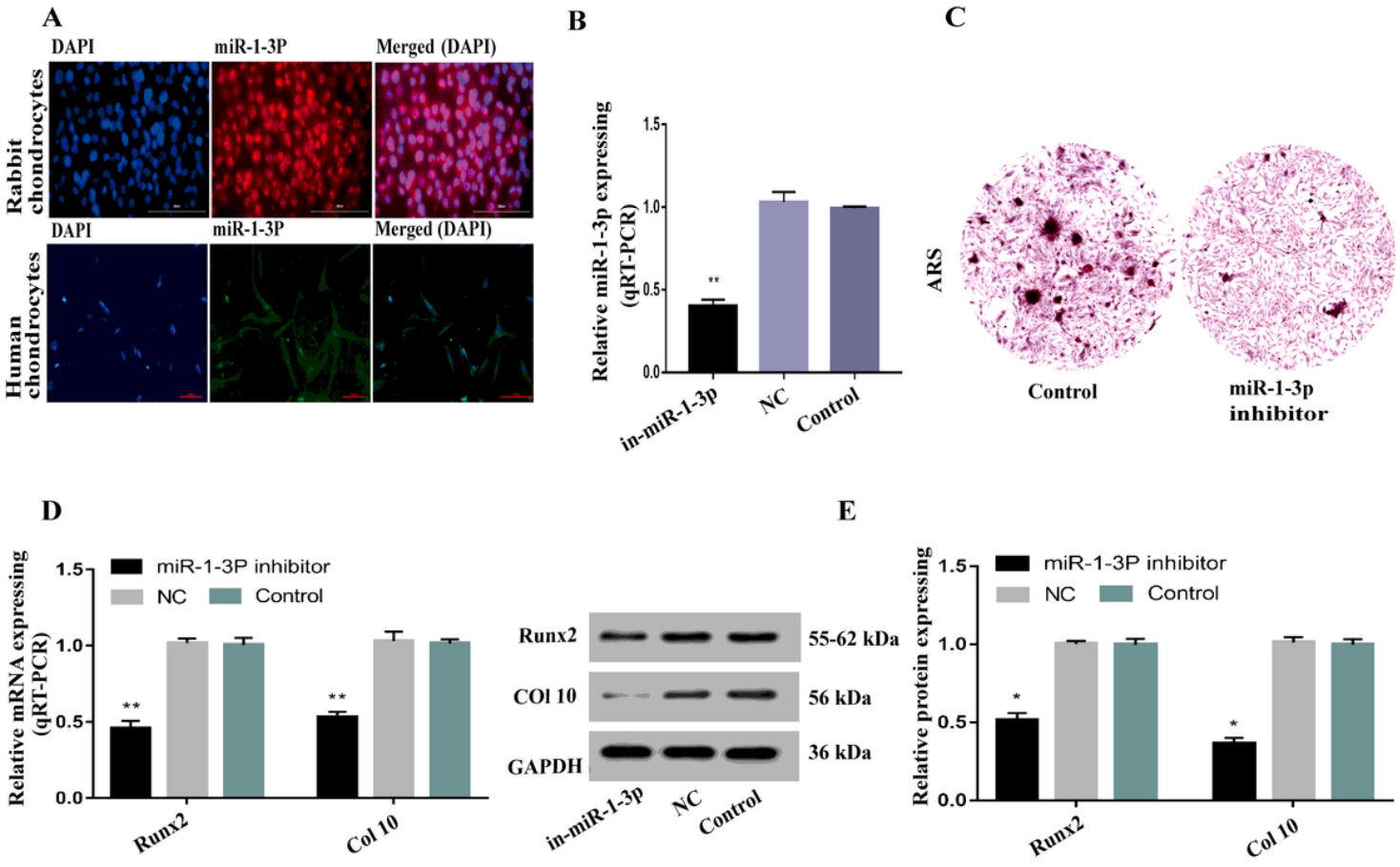

Figure 3

MiR-1-3p downregulation suppresses chondrocytes hypertrophy and reduces mineralization (A) FISH was used to verify miR-1-3p expression in rabbit and human chondrocytes (a). Scale bar: 100 μm. (B) Introduction of miR-1-3p inhibitor successfully downregulated miR-1-3p levels in human chondrocytes. (C) ARS Staining of mir-1-3p downregulated chondrocytes exhibiting reduced mineralization, as compared to controls. Scale bar: 200 μm. (D-E) Reduced RUNX2 and collagen type X levels in miR-1-3p-silenced chondrocytes verses controls. (*P<0.05, **P<0.01)

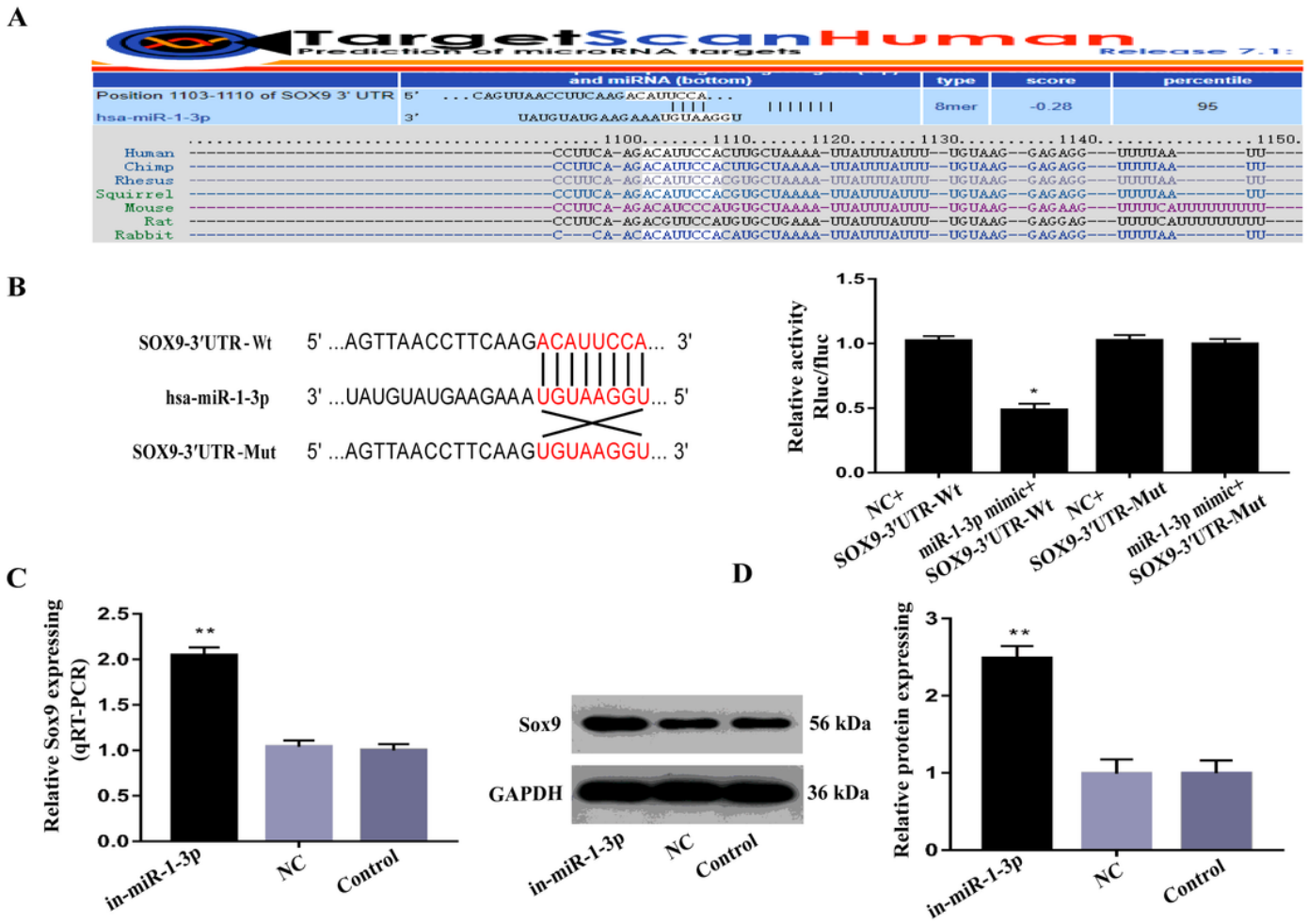

Figure 4

MiR-1-3p directly targets SOX9 in human chondrocytes (A) Bioinformatics database analysis showing miR-1-3p directly targets SOX9. (B) Luciferase reporter assay verifying the interaction between miR-1-3p and SOX9. (C-D) Evaluation of SOX9 transcript and protein expression in miR-1-3p inhibitor or NC-miRNA inhibitor treated chondrocytes. (*P<0.05, **P<0.01).

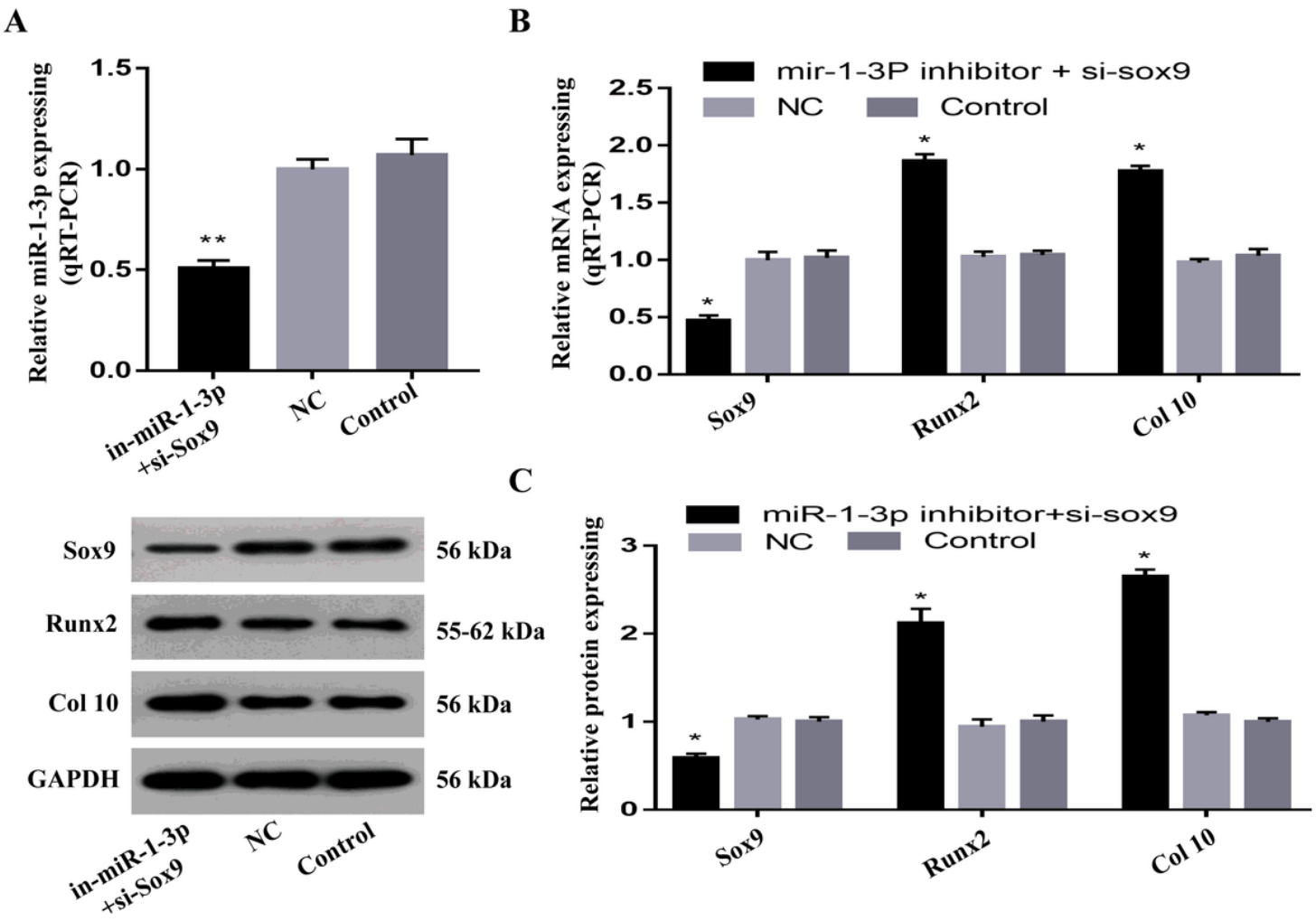

Figure 5

SOX9 silencing rescued the effects of low miR-1-3p on chondrocytes differentiation (A) Evaluation of mir-1-3p levels after the simultaneous incorporation of mir-1-3p inhibitor and si-sox9 in chondrocytes. (B-C) Evaluation of SOX9, RUNX2, and collagen type X transcript and protein expressions in miR-1-3p- and SOX9-silenced chondrocytes showing downregulation of SOX9 and simultaneous upregulation of RUNX and collagen type X expression. (*P<0.05, **P<0.01).

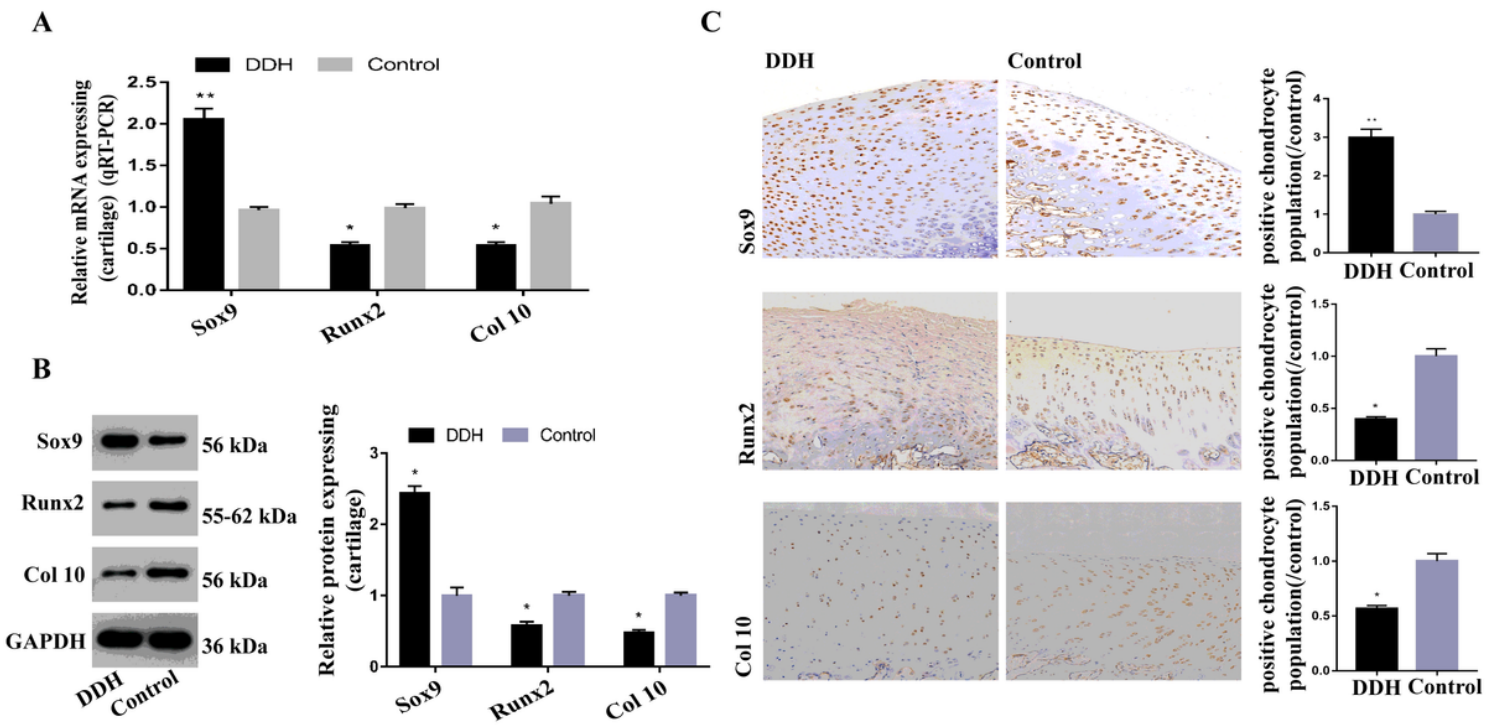

Figure 6

Verification of SOX9, RUNX2, and collagen type X expression in ARC of DHH rabbits (A-C) Using qPCR, western blot analysis, and immunohistochemistry, SOX9 levels were shown to be high and RUNX2 and collagen type X levels low in DDH ARC specimens, as opposed to controls. (*P<0.05, **P<0.01).